TELKOMNIKA Telecommunication Computing Electronics and Control
Vol. 23, No. 4, August 2025, pp. 857~870
ISSN: 1693-6930, DOI: 10.12928/TELKOMNIKA.v23i4.26727

Modified electro-optical modulator based bipolar optical code division multiple access for free-space optics

Eddy Wijanto[1,2], Kevin Sutanto[1]
[1]Department of Electrical Engineering, Faculty of Engineering and Computer Sciences, Universitas Kristen Krida Wacana, Jakarta, Indonesia
[2]Sustainable Eco-Smart Digital Infrastructure Center, Universitas Kristen Krida Wacana, Jakarta, Indonesia

Article Info

Article history:

Received Oct 14, 2024
Revised Apr 12, 2025
Accepted May 10, 2025

Keywords:

Atmospheric turbulence
Bipolar code
Electro-optical modulator
Free-space optics
Optical code division multiple access
Polarization division multiplexing
Spectral amplitude coding

ABSTRACT

This study introduces a modified electro-optical modulator (EOM) to enhance bipolar optical code division multiple access (OCDMA) in free-space optical (FSO) communication. The proposed system improves signal quality, spectral efficiency, and resilience to atmospheric turbulence. Unlike conventional dual EOM techniques, the modified EOM enables simultaneous transmission of ‘0’ and ‘1’ chip values, reducing multiple access interference (MAI) and enhancing system robustness. This approach optimizes bandwidth utilization and ensures stable performance in varying environmental conditions. Simulations were conducted in an additive white Gaussian noise (AWGN) channel using three spectral amplitude coding (SAC) schemes: modified M-sequence, Walsh-Hadamard, and random diagonal (RD) codes. Results indicate that the modified EOM scheme significantly improves FSO system performance, achieving an average 47.1% lower minimum log of bit error rate (BER) in normal weather and 43.3% lower in extreme weather, ensuring superior noise suppression and signal integrity across varying environmental conditions. Additionally, the system maintains superior performance over longer distances, demonstrating its suitability for high-speed, long-range FSO applications. These findings highlight the potential of the modified EOM-based bipolar OCDMA system in advancing next-generation optical wireless networks, offering a more efficient, interference-resistant, and high-capacity communication solution for future technologies such as 6G and beyond.

Corresponding Author:

Eddy Wijanto
Department of Electrical Engineering, Faculty of Engineering and Computer Sciences
Universitas Kristen Krida Wacana, Jakarta, Indonesia
Email: eddy.wiyanto@ukrida.ac.id

1. INTRODUCTION

The evolution of wireless communication has seen a steady transition from 5G to 6G, driven by the increasing demand for ultra-fast, highly reliable wireless connectivity [1]. 6G networks aim to integrate artificial intelligence, quantum computing, and enhanced security features to support applications such as smart cities, autonomous vehicles, and large-scale internet of things (IoT) networks. Free-space optical (FSO) communication has emerged as a promising solution to complement radio frequency-based systems, offering higher data rates, improved security, and immunity to electromagnetic interference [2]. Lu and Zheng [3] emphasized that 6G will integrate artificial intelligence (AI), blockchain, and data analytics to develop intelligent, seamless, and secure communication networks. These networks will address diverse industry needs while ensuring high-speed and reliable connectivity. Optical fiber plays a crucial role in 6G by offering high bandwidth and low latency, making it essential for applications such as cloud computing, IoT, and highdefinition streaming. Unlike radio frequency (RF) communication, optical fiber transmits data using light signals through glass or plastic strands, ensuring minimal interference, high-speed transmission, and improved security [4].

While optical fiber provides a robust solution for high-capacity data transmission, optical wireless communication (OWC) and free-space optics (FSO) serve as wireless alternatives where fiber deployment is impractical. These systems use light for wireless data transmission, offering higher bandwidth and lower latency than RF while being immune to electromagnetic interference. However, challenges such as sensitivity to atmospheric conditions and precise transceiver alignment persist. Despite these limitations, advances in multi-modal FSO systems have enabled 60 Gbps transmission over 3,600 meters using orthogonal frequency division multiplexing (OFDM) and diagonal permutation shift-optical code division multiple access (DPS-OCDMA) [5]. Additionally, hybrid optical fiber communication (OFC)-FSO systems with spectral amplitude coding (SAC)-OCDMA maintain stable performance in foggy environments [6]. Optical beam stabilization techniques, such as lens-based stabilization with 3-axis voice-coil motors (VCMs), further improve FSO reliability by achieving error-free transmission over 200 meters [7]. Meanwhile, turbulence simulation models have been developed to assess FSO performance under extreme conditions [8].

FSO technology has also evolved for specific applications, such as high-speed transportation and urban infrastructure. A dual-transceiver FSO system for high-speed trains was introduced, reducing the need for base stations while improving coverage in smart cities [9]. An adaptive power transmission method based on channel correlation has demonstrated significant bit error rate (BER) improvements in FSO communication, outperforming fixed threshold techniques [10], [11]. Studies also explore FSO as an alternative to sub-terahertz (THz) bands in next-generation cellular networks, addressing challenges like solar interference and beam alignment [12]. Moreover, a polarization division multiplexing (PDM) FSO system with enhanced double weight (EDW) codes has been developed, enabling 60 Gbps transmission across six channels with resilience to adverse weather conditions [13].

Multiplexing techniques play a crucial role in optimizing bandwidth efficiency in FSO communication. Frequency division multiplexing (FDM), time division multiplexing (TDM), wavelength division multiplexing (WDM), and OCDMA are widely used. A 4-bands coherent FDM passive optical network (PON) system demonstrated a total data rate of 100 Gbps, proving its potential for high-speed networks [14]. Similarly, an interleaved single-carrier FDM (I-SC-FDM) scheme integrated with a sparse weight-initiated deep neural network (SWI-DNN) equalizer achieved 660 Mbps transmission over 90 meters, reducing peak to average power ratio (PAPR) and computational complexity [15]. TDM optimizes time slots for signal transmission, though it requires precise synchronization to avoid latency. The delay-controlled and energy-efficient TDM access (DEC-TDMA) mechanism reduces delays and improves energy efficiency in fiber-wireless (FiWi) networks [16]. Meanwhile, WDM enhances FSO capacity by enabling multi-wavelength transmission, with a two-dimensional photodetector array (2D-PDA) system achieving 100 Gbps [17]. A bidirectional WDM-FSO system for data centers demonstrated 320 Gbps transmission over 1,000 meters using reflective semiconductor optical amplifiers (RSOAs) to reduce costs while maintaining high-speed communication [18]. Another hybrid WDM-FSO system achieved 32 Gbps over 100 meters, proving its potential for cost-effective, high-speed light-based Wi-Fi solutions [19].

OCDMA assigns unique optical codes to users, optimizing bandwidth efficiency but facing multiple access interference (MAI). A flexible double-weight (FDW) code supported over 220 users at 2.5 Gb/s over 60 km, reducing MAI [20]. Additionally, a hybrid spectral/spatial OCDMA system integrating OFDM and successive weight (SW) coding achieved 1.5 Tb/s capacity with 350-user support [21]. Further refinements in OCDMA include coherent and non-coherent approaches. Coherent OCDMA improves spectral efficiency through phase encoding but requires precise synchronization, while non-coherent methods use intensity-based encoding, offering simpler implementation [22]. The 3D multi-diagonal (MD) code is a strong candidate for high-throughput networks, providing higher data rates and increased user capacity [23]. SAC-OCDMA enhances security and scalability, with innovations like one-dimensional two-distinct codes with two-code keying (TCK) reducing multiple user interference while supporting 45 users at 2.5 Gbps [24]. Another approach, the multi-dimensional sigma shift matrix (nD-SSM) code, improves BER and increases capacity at higher data rates [25].

Polarization-based encoding in FSO further enhances security and resilience against turbulence. Polarization-encoded signals maintain integrity even in highly scattering environments like underwater bubbles, making them suitable for long-range communication [26]. Studies have shown that bipolar OCDMA with fiber Bragg gratings (FBG) effectively suppresses MAI while improving transmission stability [27]. Meanwhile, bipolar OCDMA with SAC and polarization coding has been demonstrated to enhance transmission rates and MAI suppression in FSO systems [28]. Simulations indicate that Walsh–Hadamard codes perform best under extreme weather conditions, while MD codes are more effective for medium-range distances. While bipolar OCDMA systems have been extensively studied for enhancing spectral efficiency and reducing interference in FSO communication, existing implementations suffer from limitations such as MAI and reduced performance over long distances. Traditional dual electro-optical modulator (EOM) systems only transmit one chip value at a time, leading to inefficiencies in data transmission. Our proposed modified EOM technique addresses these challenges by enabling simultaneous transmission of both chip values, thereby enhancing signal integrity and overall system robustness.

The improved bipolar OCDMA system using the modified EOM technique has wide-ranging applications in various real-world scenarios. It can enhance urban wireless networks by providing high-speed communication in densely populated areas, support satellite communication by ensuring secure, long-distance optical links, and facilitate IoT integration by enabling efficient data transmission in smart infrastructure applications. These contributions position our study as a significant advancement in the field of optical wireless communication.

Building upon these advancements, this paper presents several key contributions to the field of optical communications: (i) the paper introduces a novel modulation technique based on modified EOMs for implementing bipolar OCDMA in FSO systems. This technique offers improved performance and efficiency compared to previous dual EOM methods; (ii) by employing bipolar modulation with the modified EOMs, the system achieves enhanced signal quality and robustness against various impairments, such as noise and atmospheric turbulence, encountered in FSO communication links. This improvement leads to better overall system reliability and data transmission integrity; (iii) the proposed system increases spectral efficiency by allowing multiple users to share the same optical channel concurrently using orthogonal codes. This results in optimized bandwidth utilization and higher capacity, making it suitable for high-throughput applications in FSO networks; (iv) the paper provides simulation validation of the proposed technique, demonstrating its feasibility and effectiveness in real-world FSO environments. Through comprehensive simulation testing and analysis, the performance advantages of the modified EOM-based bipolar OCDMA system are confirmed, paving the way for its practical implementation in FSO communication systems; and (v) the research presented in the paper offers valuable insights into the design and deployment of advanced optical communication systems for various practical applications, including terrestrial and satellite-based FSO links. The demonstrated improvements in performance and efficiency contribute to the advancement of FSO technology, addressing the growing demand for high-speed, reliable, and secure data transmission solutions.

2. METHOD

The simulation conducted in this study evaluated the performance of bipolar OCDMA utilizing the modified EOM scheme proposed herein. Compared to the switch scheme discussed in [27], the bipolar OCDMA with the modified EOM scheme demonstrated an increased transmission rate. Unlike the FBG-based encoding utilized in previous simulations [27], this study employed a continuous wave (CW) laser array for encoding in accordance with the signature code, with an erbium-doped fiber amplifier (EDFA) serving as a pre-amplifier. The dual EOM scheme faces a significant limitation in that it only transmits signals for chip “1” in the signature code, neglecting chip “0” [29]. While this approach simplifies the system, it results in a less comprehensive and reliable data transmission [29].

The encoding process modulates the user information signal using an EOM with a CW laser array based on the signature code. When the user information bit is “1,” only the upper EOM modulates the signal, directing it to the corresponding polarization splitter. Conversely, when the bit is “0,” the lower EOM performs the modulation. A second pair of EOMs works with the same principle but in reverse. In this case, when the user information bit is “1,” only the lower EOM transmits the signal, while the upper EOM transmits when the bit is “0.” This complementary operation ensures both polarization states are represented, enhancing data transmission and ensuring the system can handle different bit values across both channels efficiently. The polarized signals from both pairs of EOMs are combined using a polarization combiner, ensuring that all modulated signals are effectively merged. Once combined, the signals are transmitted through the FSO channel, facilitating robust and accurate data transmission. This approach enhances signal integrity by ensuring both polarization states are utilized before transmission. Figure 1 illustrates the encoder of the bipolar OCDMA with modified EOM scheme utilized in this simulation.

After passing through the FSO channel, the optical signals experienced depolarization into horizontal and vertical polarization states. These signals then traveled through either the lower or upper port #1 of the optical circulator, depending on their polarization state. From port #2 of the circulator, the optical signals entered the FBG decoder, which functioned based on the assigned signature code. The reflected optical spectra were directed to the lower optical adder through port #3 of the circulator, while signals transmitted through the FBG were directed to the upper optical adder. Following the conversion of optical to electrical signals using avalanche photo-diodes (APDs), a subtraction of the upper and lower signals was performed to achieve balanced photo-detection. Subsequently, the BER and the quality factor (Q-factor) were evaluated with a BER analyzer. Figure 2 displays the decoder of the bipolar OCDMA using a modified EOM as implemented in this simulation. For example, with the Walsh-Hadamard code used as the signature code, when the user transmitted a bit “0”, only the lower EOM modulated the signals toward the lower polarization splitter, resulting in horizontally polarized signals traversing the FSO channel. At the receiver, these signals were depolarized into the lower optical circulator. As the lower circulator was linked to the complementary FBG, the signals proceeded to the lower APD, leaving the upper APD signal-free. This process generated negative signals corresponding to “-1” in the bipolar setup. In contrast, when a bit “1” was sent, the signals appeared in the upper APD with no signal in the lower APD, producing positive signals equivalent to “+1” in the bipolar scheme. The approach was extended to multi-user scenarios by applying the same design methodology. Incorporating signature codes of length N into the proposed designs required calculating the correlation outcomes, where variables n and m represented the optical codewords for horizontal and vertical polarization states, respectively, which is presented in (1) and (2).

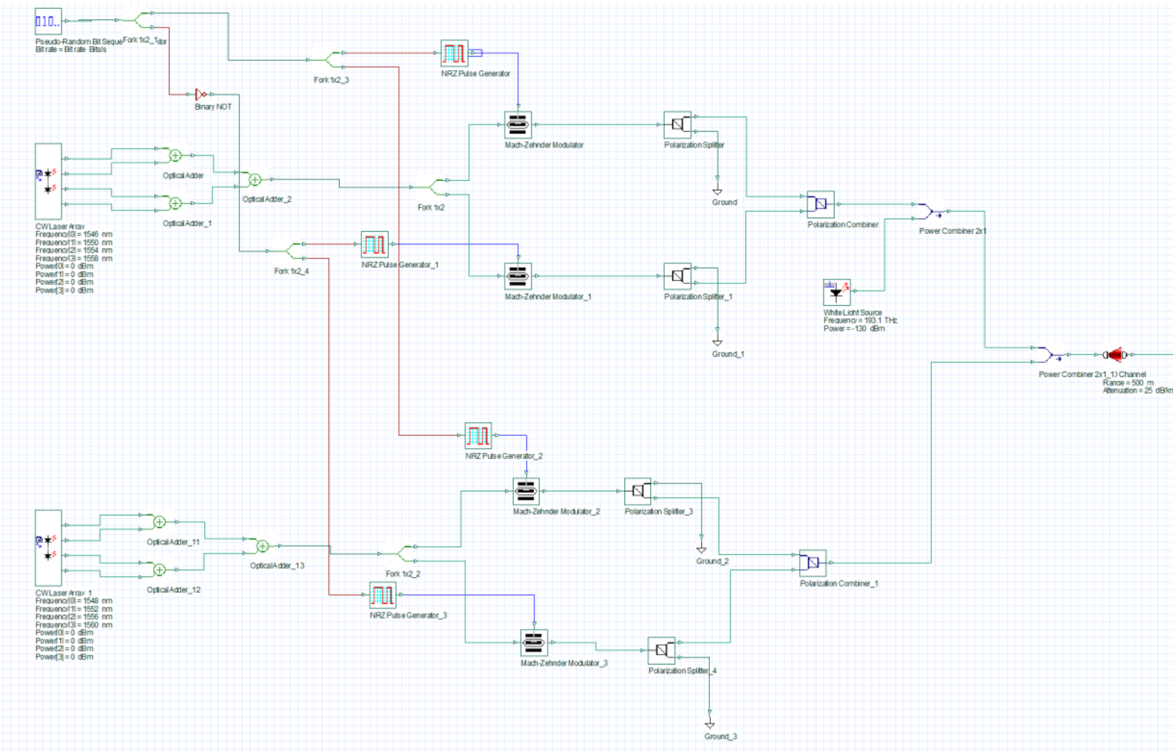

Figure 1. Bipolar OCDMA with modified EOM scheme encoder

$$R_{XX}^{(nm)}(j,k)=\sum_{i=1}^{N} x_j^{(n)}(i)x_k^{(m)}(i)=\begin{cases}(N+1), \text{for } j=k \text{ and } n=m\\ \frac{(N+1)}{2}, \text{for } j\neq k \text{ and } n=m\\ 0 \quad , \quad \text{otherwise}\end{cases} \quad (1)$$

$$R_{XX}^{(nm)}(j,\overline{k})=\sum_{i=1}^{N} x_j^{(n)}(i)\left[1-x_k^{(m)}(i)\right]=\begin{cases}\frac{(N+1)}{2}, \text{for } j\neq k \text{ and } n=m\\ 0 \quad , \quad \text{otherwise}\end{cases} \quad (2)$$

The performance analysis was first carried out in an additive white Gaussian noise (AWGN) channel environment, using three different codes and applying both the dual EOM and modified EOM schemes. Further simulations were then performed in the AWGN channel to compare the performance of each code within each scheme. Additionally, performance analysis was conducted under extreme weather conditions to evaluate the system’s resilience and reliability in real-world scenarios.

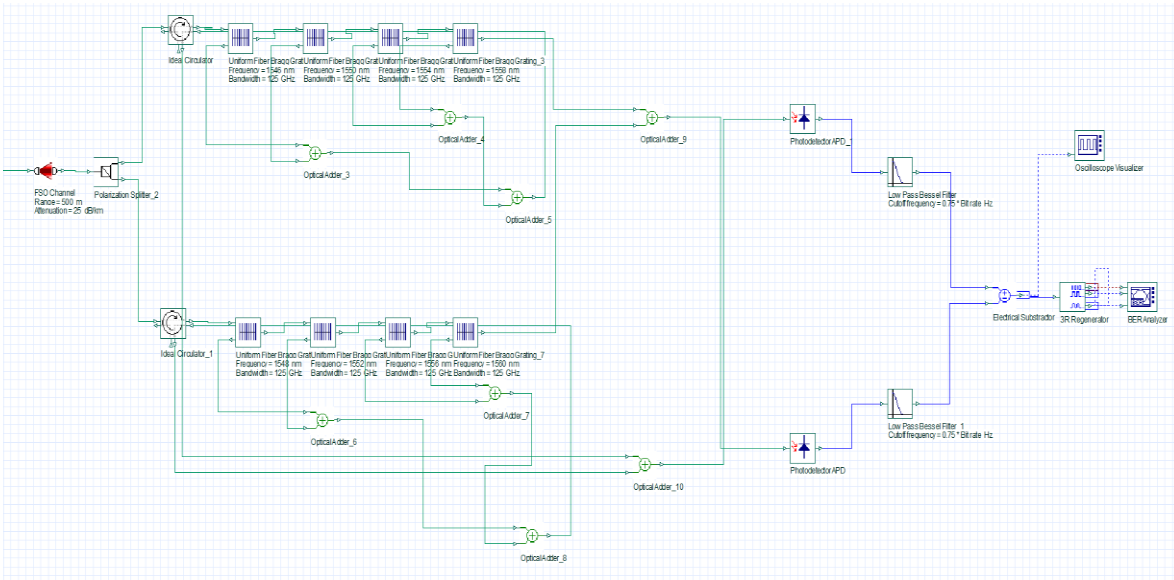

Figure 2. Bipolar OCDMA with modified EOM scheme decoder

The evaluation of the performance of bipolar OCDMA using the modified EOM scheme was carried out based on the simulation parameters outlined in Table 1. In the simulation, three SAC-OCDMA codes specifically, the modified M-sequence (MS) code [28], walsh-hadamard (WH) code, and random diagonal (RD) code—were utilized. These codes satisfy the correlation properties described in (1) and (2), demonstrating their compatibility with the bipolar OCDMA employing the modified EOM scheme. The signature codes for two users employed in simulation are detailed in Table 2.

Table 1. Simulation parameters

Parameter		Value
Global	Bit rate	10e+009 bits/s
	Sample rate	640e+009 Hz
	Number of samples	4096
CW laser	Linewidth	10 MHz
	Power	0 dBm
	Azimuth	45 deg
	Wavelength	1546…1560 nm ($\lambda_1 \ldots \lambda_8$)
Mach-Zehnder modulator	Extinction ratio	30 dB
	Symmetry factor	-1
Uniform FBG	Bandwidth	125 GHz
	Reflectivity	0.99
	Noise threshold	−100 dB
Avalanche photodetector	Gain	3
	Responsivity	1 A/W
	Ionization ratio	0.9
	Dark current	10 nA
	Sample rate	5*(sample rate)
	Thermal power density	100e-024 W/Hz
FSO channel	Range	50–500 m
	Transmitter aperture diameter	5 cm
	Receiver aperture diameter	20 cm
	Beam divergence	2 mrad

Table 2. Signature codes

Code	Signature code
Modified M-Sequence	$\begin{bmatrix} 1 & 0 & 1 & 1 & 1 & 0 & 0 & 0 \\ 1 & 1 & 1 & 0 & 0 & 1 & 0 & 0 \end{bmatrix}$
Walsh-Hadamard	$\begin{bmatrix} 1 & 0 & 1 & 0 & 1 & 0 & 1 & 0 \\ 1 & 1 & 0 & 0 & 1 & 1 & 0 & 0 \end{bmatrix}$
RD	$\begin{bmatrix} 1 & 0 & 0 & 1 & 0 & 1 & 1 & 0 \\ 0 & 0 & 1 & 0 & 1 & 1 & 1 & 0 \end{bmatrix}$

The assessment was based on evaluating the BER and the Q-factor of the system. The BER can be calculated using the formula given in [30].

$$BER = \frac{1}{2} erfc\left(\sqrt{\frac{SNR}{2}}\right) \tag{3}$$

where *SNR* represents the signal-to-noise ratio of the proposed system, and signifies the complementary error function over time, which can be calculated as (4) [31]:

$$erfc = \frac{2}{\sqrt{\pi}} \int_x^\infty exp(-t^2)\, dt \tag{4}$$

In this simulation, to simplify the analysis, we utilized the minimum logarithm of the BER, which can be obtained as outlined in reference [32].

$$min\{l\, og(BER)\} = log_{10} B\, ER \tag{5}$$

The correlation between the BER and Q-factor can be computed as described in references [33], [34].

$$BER = \frac{1}{2} erfc\left(\frac{Q}{\sqrt{2}}\right) \tag{6}$$

3. RESULTS AND DISCUSSION

The simulation employed OptiSystem version 10, a respected optical system application. It evaluated the effectiveness of the proposed modified EOM scheme in comparison with the existing dual EOM scheme. This assessment was conducted using the configurations shown in Figures 1 and 2, focusing specifically on a multi-user scenario.

Figure 3(a) present output data in the context of the dual EOM scheme, utilizing the Walsh-Hadamard code for a single user. The corresponding received signals illustrate amplitude variations within the micro a.u. range, providing insight into the performance characteristics of the dual EOM configuration. The signal waveform demonstrates a relatively lower intensity, which may impact the system’s robustness in terms of BER and Q-Factor, particularly in challenging transmission environments. Figure 3(b) similarly illustrate output data which is obtained under the modified EOM scheme, also employing the Walsh-Hadamard code for a single user. Unlike the dual EOM configuration, the received signals in this scheme exhibit significantly higher amplitude values, measured within the hundred-micro a.u. range. The increased signal intensity indicates a more efficient signal transmission process, reducing the likelihood of signal degradation and enhancing overall system performance in terms of signal clarity and reliability.

The modified EOM scheme generates a stronger output signal compared to the dual EOM scheme. This enhanced signal intensity suggests that the modified EOM configuration offers superior performance in BER and Q-Factor, as a higher signal amplitude generally results in better resilience against noise, reduced signal distortion, and improved detection accuracy at the receiver. The modified EOM approach holds significant advantages for OWC and FSO systems, particularly in environments where signal attenuation and interference pose challenges to maintaining high transmission quality.

Furthermore, the observed differences in signal intensity underscore the modified EOM scheme’s potential for higher system efficiency and scalability. The increased amplitude of the received signals suggests that this scheme can maintain stable performance over longer distances, making it a promising solution for applications requiring high-speed, long-range optical communication. The Walsh-Hadamard code, known for its orthogonality and ability to minimize MAI, further complements the advantages of the modified EOM scheme by ensuring efficient spectral utilization and enhanced signal integrity. Overall, the comparison of Figures 3(a) and 3(b) demonstrate that the modified EOM scheme not only achieves greater signal amplitude but also improves signal robustness and quality, contributing to lower BER and higher Q-Factor. This makes it a more viable and efficient choice for next-generation optical networks, including 6G and beyond, where high data rates, low-latency communication, and resilience against external disturbances are crucial.

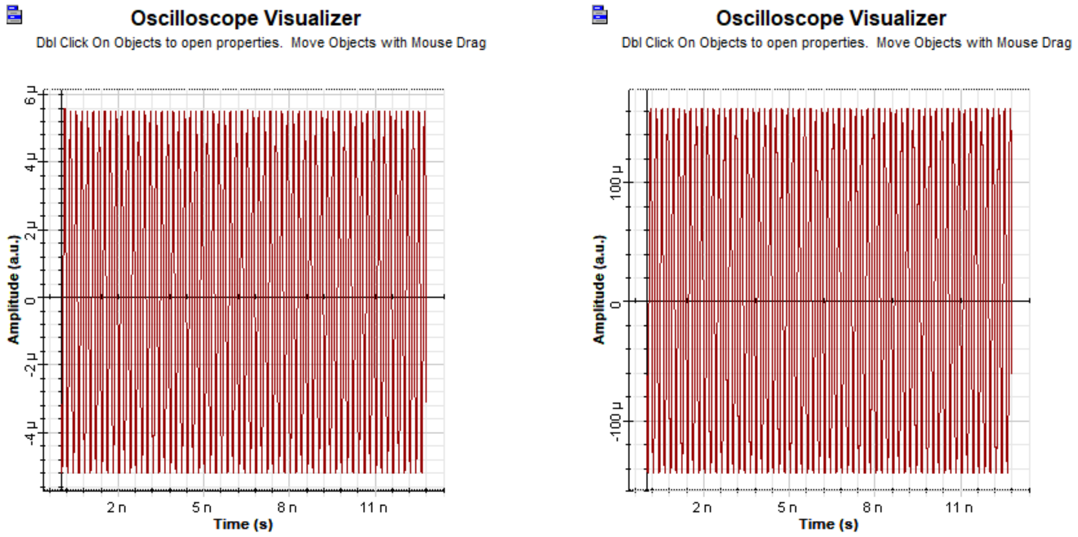

(a) (b)

Figure 3. Output of the bipolar OCDMA utilizing configuration of (a) dual EOM and (b) modified EOM

The effectiveness of the MAI reduction feature was evaluated under incompatible conditions. Specifically, an incompatible decoder was employed with the encoder in the context of the modified EOM scheme. This scheme utilized signature codes from the Walsh-Hadamard set: (1010) for user #1 and (1100) for user #4. Figure 4 displays the output observed after detection in instances where an incompatible decoder was employed and bit “0” was transmitted. Additionally, a minor noise-floor signal was detected due to the imperfect filtering of the FBG decoder. These results proof the MAI cancellation feature of the proposed scheme.

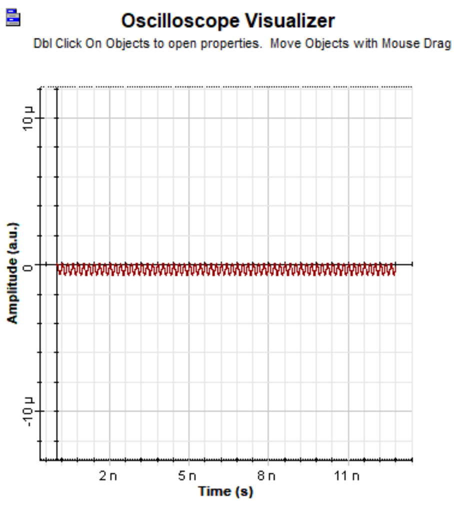

Figure 4. Output of bipolar OCDMA with modified EOM scheme for incompatible condition

Further simulation involved the application of a multi-user bipolar OCDMA utilizing the modified EOM scheme across various SAC codes under AWGN channel conditions for normal and extreme weather condition. Performance evaluation was conducted, presenting results in terms of the minimum logarithm of the BER and the maximum Q-factor. Figure 5 illustrates the performance of the proposed modified EOM based OCDMA system in an AWGN channel under normal and extreme weather condition using three different codes. Examining Figure 5(a), WH and RD codes exhibit the best performance with the lowest minimum Log of BER, whereas Modified MS codes perform the weakest. At a transmission range of 500 meters, WH codes achieve a 10.21% lower BER than RD codes and 16.15% lower BER than Modified MS codes, confirming their superior efficiency in an AWGN environment. The minimum Log of BER under extreme weather conditions shows notable performance degradation across all codes. WH and RD codes sustain relatively lower BER values compared to Modified MS, which experiences the highest degradation. Under heavy fog conditions, RD codes exhibit a 9.08% higher BER compared to WH codes, while Modified MS suffers a 16.30% increase in BER degradation. Meanwhile, Figure 5(b) illustrates the maximum Q-Factor achieved using the modified EOM scheme. WH codes lead with a 7.32% Q-Factor improvement over RD codes and 9.36% over Modified MS codes. As the transmission distance increases, WH continues to outperform RD, demonstrating its resilience in maintaining signal integrity. These results confirm that WH codes consistently deliver the most reliable performance, while Modified MS struggles the most under standard AWGN conditions. The maximum Q-Factor in extreme weather conditions reinforces these observations. WH codes achieve the highest Q-Factor, maintaining a 4.94% advantage over RD and 9.34% over Modified MS at longer transmission distances. Over extended ranges, WH remains the most robust against environmental disruptions, confirming its reliability for challenging weather scenarios. In contrast, Modified MS proves to be the least stable, exhibiting substantial performance losses of up to 20.00% in extreme conditions.

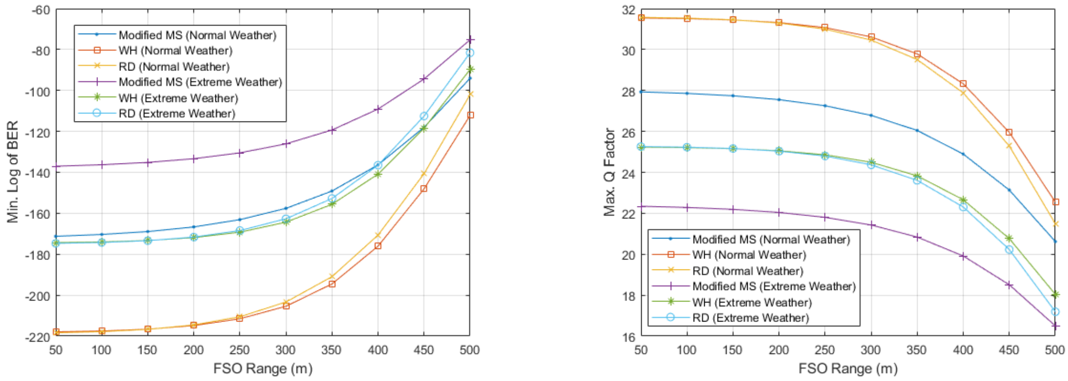

(a) (b)

Figure 5. Performance analysis of bipolar OCDMA with a modified EOM configuration in an AWGN channel under normal and extreme weather condition: (a) min. log of BER and (b) max. Q-factor

In the final simulation, the performance of each code was compared using both the dual EOM and modified EOM schemes under AWGN channel conditions for normal and extreme weather condition. Figure 6(a) compares the performance of WH codes in both the dual EOM and modified EOM schemes under AWGN conditions. It is evident that the modified EOM scheme significantly outperforms the dual EOM scheme. The minimum Log of BER for WH codes in the modified EOM scheme is 61.37% lower than in the dual EOM scheme at a range of 500 meters. This indicates a substantial improvement in signal quality and efficiency with the modified EOM technique. When evaluating performance under extreme weather conditions for WH codes, the modified EOM scheme again demonstrates superior performance. The minimum Log of BER in the modified EOM scheme is 54.58% lower compared to the dual EOM scheme under extreme weather conditions. This shows that the modified EOM system is better equipped to handle environmental disturbances. Figure 6(b) further emphasizes this advantage, as the maximum Q-Factor for WH codes in the modified EOM scheme is 100.38% higher than that achieved with the dual EOM scheme under normal weather conditions. These results demonstrate the superiority of the modified EOM scheme in enhancing signal integrity and reducing interference. The maximum Q-Factor also confirms that the modified EOM scheme outperforms the dual EOM scheme by 128.88% in extreme weather. This highlights the enhanced robustness of the modified EOM system, making it more reliable for high-capacity FSO networks, particularly in real-world applications with challenging weather conditions.

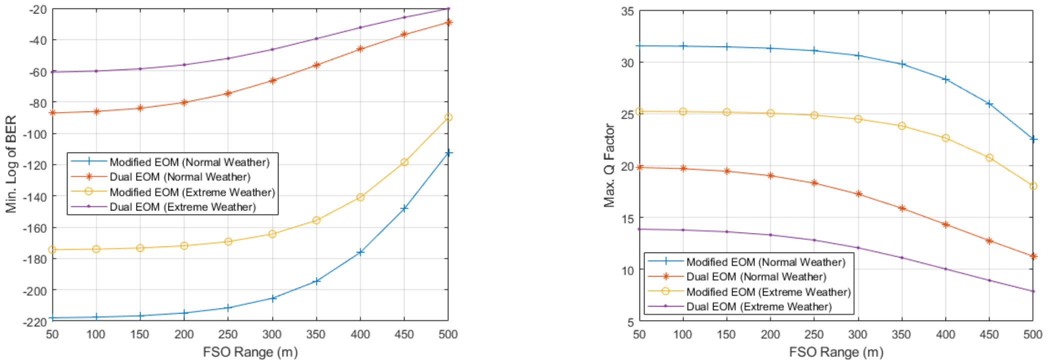

(a) (b)

Figure 6. Performance comparation of bipolar OCDMA with dual EOM and modified EOM scheme in AWGN channel under normal and extreme weather condition for WH codes: (a) min. log of BER and (b) max. Q-factor

In Figure 7(a), which compares the performance of RD codes in both the dual EOM and modified EOM schemes under AWGN conditions, the modified EOM scheme demonstrates significant improvement. The minimum Log of BER for RD codes in the modified EOM scheme is 51.13% lower than in the dual EOM scheme at a transmission range of 500 meters, indicating better noise resilience and interference suppression. For RD codes under extreme weather conditions, the modified EOM scheme maintains its advantage despite increased atmospheric disturbances. The minimum Log of BER in the modified EOM scheme is 72.74% lower than in the dual EOM scheme under extreme weather conditions, proving its robustness in harsh environments. Meanwhile, Figure 7(b) shows that the maximum Q-Factor for RD codes in the modified EOM scheme is 23.40% higher than in the dual EOM scheme, reinforcing the enhanced signal quality achieved with this method. These findings confirm that RD codes benefit significantly from the modified EOM scheme, leading to better overall system performance in an AWGN channel. For the maximum Q-Factor performance, RD codes in the modified EOM scheme achieve a 41.74% higher Q-Factor compared to the dual EOM scheme. This significant improvement suggests that the modified EOM scheme ensures better signal integrity and stability even under adverse weather conditions, making it more suitable for practical deployment in real-world FSO communication systems.

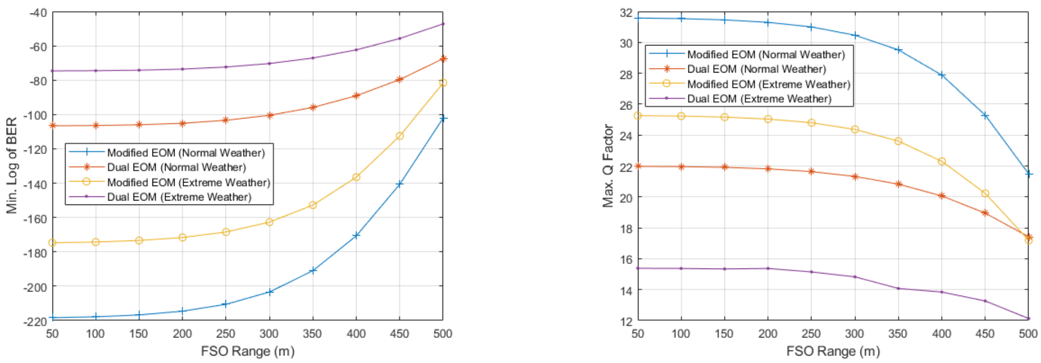

(a) (b)

Figure 7. Performance comparation of bipolar OCDMA with dual EOM and modified EOM scheme in AWGN channel under normal and extreme weather condition for RD codes: (a) min. log of BER and (b) max. Q-factor

A closer look at Figure 8(a) reveals that the modified M-sequence (MS) codes benefit significantly from the modified EOM scheme in AWGN conditions. The results indicate a 131.41% lower minimum Log of BER compared to the dual EOM scheme at a 500-meter transmission range, demonstrating superior noise suppression. Under extreme weather conditions, performance degradation becomes more evident, but the modified EOM scheme maintains a 164.45% lower BER than the dual EOM scheme despite increased atmospheric disturbances. This improvement indicates a higher resilience to environmental variations. Meanwhile, Figure 8(b) presents a 53.66% improvement in the maximum Q-Factor, confirming enhanced signal clarity and reliability when using the modified EOM scheme. These findings highlight the advantages of the modified EOM approach in improving the performance of Modified MS codes in standard FSO environments. The maximum Q-Factor in extreme weather remains 75.58% higher for the modified EOM scheme, reinforcing its ability to sustain signal integrity even under challenging conditions. These results confirm that the modified EOM-based bipolar OCDMA system is better suited for real-world FSO applications, ensuring reliable communication across varying operational environments.

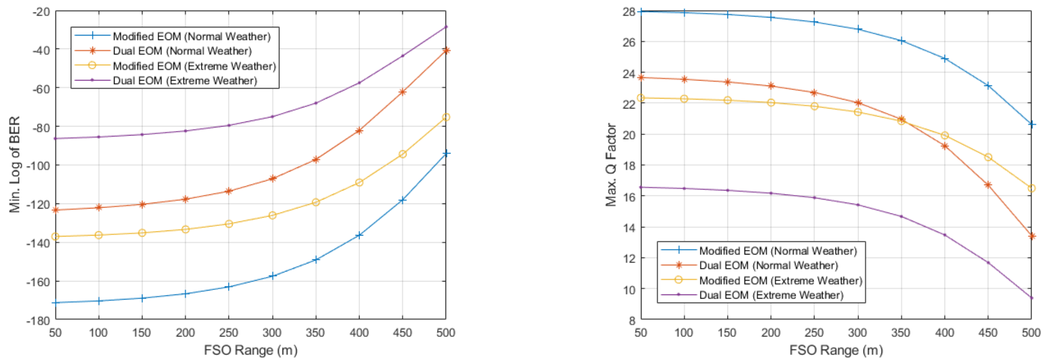

(a) (b)

Figure 8. Performance comparation of bipolar OCDMA with dual EOM and modified EOM scheme in AWGN channel under normal and extreme weather condition for Modified MS codes: (a) min. log of BER and (b) max. Q-factor

In bipolar OCDMA systems, the analysis of eye diagrams serves as a critical means of assessing signal quality and integrity [35]. Comparing the performance of the eye diagrams between systems employing the modified EOM scheme and those using the dual EOM scheme reveals significant advantages for the former. The superiority of the modified EOM scheme stems from its ability to transmit signals corresponding to both chips “0” and “1” within the signature code, thereby offering a more comprehensive representation of the transmitted data. In contrast, the dual EOM scheme exclusively transmits signals corresponding to chip “1” in the signature code, leading to a less nuanced depiction in the eye diagram. As a result, the eye diagram in the modified EOM scheme exhibits clearer and more distinct eye openings, indicating enhanced signal clarity and reduced distortion. This improvement is illustrated in Figure 9, where Figure 9(a) shows the eye diagram for the dual EOM configuration and Figure 9(b) presents the eye diagram for the modified EOM scheme. This clarity translates into improved system performance metrics such as reduced BER and higher Q-factor. Consequently, in bipolar OCDMA systems, the use of the modified EOM scheme proves superior to the dual EOM scheme, ensuring more reliable and efficient communication networks.

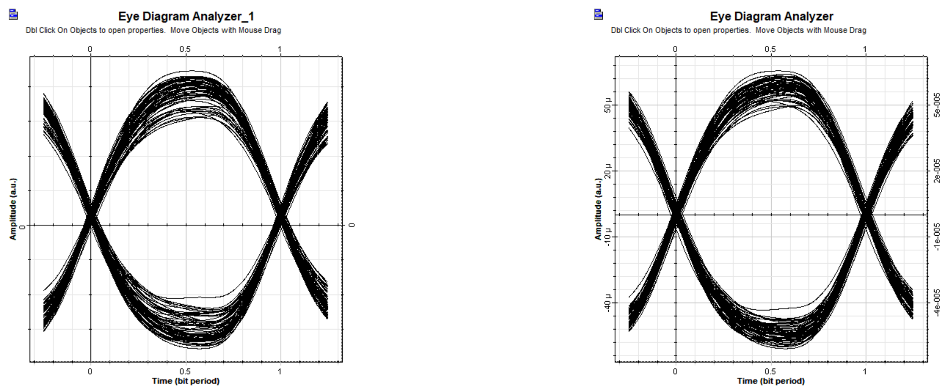

(a) (b)

Figure 9. Eye diagram of bipolar OCDMA: (a) dual EOM and (b) modified EOM

The modified EOM-based bipolar OCDMA system offers significant advancements over existing bipolar modulation techniques, particularly in polarization coding for wireless optical communication. While phase modulator-based approaches enhance spectral efficiency, they are highly sensitive to phase noise and polarization mode dispersion, making them less reliable in turbulent FSO environments [27]. In contrast, the modified EOM technique employs intensity-based bipolar modulation, which is more resilient to phase distortions, improves MAI suppression, and enhances overall system robustness. Integrating SAC further simplifies implementation, making the system more scalable and interference-resistant for large-scale FSO deployments.

Scalability, however, remains a challenge, as increasing the number of users can lead to higher MAI, greater computational complexity, and signal degradation over long distances. Advanced coding techniques, hybrid spectral/spatial OCDMA, dynamic code allocation, and OFDM integration can enhance spectral efficiency and user separation. Moreover, machine learning-based resource management, adaptive beam steering, and hybrid FSO-fiber systems can improve reliability. While simulations show significant enhancements in BER and Q-factor for limited-user scenarios, experimental validation under diverse conditions—including extreme weather scenarios—is crucial for large-scale deployment. Synchronization and interference management are also critical for maintaining reliable performance in large-scale FSO systems. Variations in propagation delays, atmospheric conditions, and hardware inconsistencies necessitate precise time synchronization using optical clock recovery, adaptive algorithms, and phase-locked loops (PLLs). The modified EOM system reduces MAI using orthogonal codes, but as user numbers grow, additional techniques like interference cancellation and polarization-based multiplexing are needed. Dynamic resource allocation, including adaptive power control and machine learning-based bandwidth distribution, can further optimize performance, ensuring stable communication under challenging conditions.

The implementation of the modified EOM system in FSO communication offers enhanced spectral efficiency and signal robustness but also presents technical challenges. The system relies on a CW laser array with a 0 dBm output, Mach-Zehnder modulators with a 30 dB extinction ratio, an EDFA for signal boosting, and APDs for efficient signal decoding. The FSO transceiver features a 5 cm transmitter and a 20 cm receiver aperture, with a beam divergence of 2 mrad, enabling effective transmission over distances of 50 to 500 meters. However, system costs and energy consumption remain key obstacles. Maintaining optical stability requires adaptive mechanisms and regular calibration, while integration with existing infrastructure must address thermal noise and multipath interference.

Compared to OFDM, which optimizes spectral utilization through orthogonal subcarriers but suffers from high PAPR and computational complexity, the modified EOM-based system provides a more efficient alternative for high-density communication. However, its lack of frequency diversity may limit performance under dynamic channel conditions. A hybrid approach combining OFDM with the modified EOM-based bipolar OCDMA system could improve scalability and interference resistance by leveraging OFDM’s frequency diversity while maintaining OCDMA’s efficient coding structure.

Future research should focus on experimental validation under extreme weather conditions, improving synchronization techniques, and developing adaptive interference management strategies. Additionally, practical field trials will be essential to bridge the gap between theoretical simulations and real-world deployment, ensuring the system’s feasibility for next-generation high-capacity optical networks.

4. CONCLUSION

This study presents a novel approach to enhancing FSO communication through a modified EOM in OCDMA systems. Compared to the conventional dual EOM technique, the modified EOM improves BER reduction and Q-factor enhancement while maintaining superior performance over distances up to 500 meters, reinforcing its suitability for medium to long-range FSO applications. Beyond performance gains, the modified EOM significantly reduces MAI, ensuring greater reliability in data transmission. Further analysis under extreme weather conditions, highlights its resilience, demonstrating minimal performance degradation and strong signal integrity. These findings contribute to advancing optical communication technologies, addressing the increasing demand for high-speed, secure, and reliable wireless networks, particularly for 6G applications.

Future research should focus on scalability, testing performance with more users, and expanding extreme weather evaluations. Integrating hybrid modulation techniques, such as OFDM, could further optimize spectral efficiency and system resilience. Practical field trials will be essential for validating real-world applicability. Potential applications include urban wireless backhaul, satellite communications, and IoT infrastructure. However, challenges like alignment sensitivity and cost-effective deployment must be addressed before commercialization. Ensuring real-world viability through field testing under extreme weather conditions will be key to bridging the gap between theoretical models and practical deployment, paving the way for more resilient high-capacity optical networks.

ACKNOWLEDGMENTS

Thanks to the support from Ukrida's Institute for Research and Community Services, we were able to perform data collection, analysis, and interpretation, which played a crucial role in enhancing the quality and impact of our research findings.

FUNDING INFORMATION

The authors would like to express their gratitude to Ukrida's Institute for Research and Community Services for funding this research under the Lecturer Research Grant Scheme (13/UKKW/LPPM-FTIK/LIT/VIII/2023).

AUTHOR CONTRIBUTIONS STATEMENT

This journal uses the Contributor Roles Taxonomy (CRediT) to recognize individual author contributions, reduce authorship disputes, and facilitate collaboration.

Name of Author	C	M	So	Va	Fo	I	R	D	O	E	Vi	Su	P	Fu
Eddy Wijanto	✓	✓	✓	✓	✓	✓		✓	✓	✓		✓		
Kevin Sutanto		✓	✓			✓		✓	✓		✓		✓	

C : **C**onceptualization
M : **M**ethodology
So : **So**ftware
Va : **Va**lidation
Fo : **Fo**rmal analysis
I : **I**nvestigation
R : **R**esources
D : **D**ata Curation
O : Writing - **O**riginal Draft
E : Writing - Review & **E**diting
Vi : **Vi**sualization
Su : **Su**pervision
P : **P**roject administration
Fu : **Fu**nding acquisition

CONFLICT OF INTEREST STATEMENT

Authors state no conflict of interest.

INFORMED CONSENT

Not applicable. This study did not involve any human participants requiring informed consent.

ETHICAL APPROVAL

Not applicable. This study did not involve human or animal subjects.

DATA AVAILABILITY

The authors confirm that the data supporting the findings of this study are available within the article.

REFERENCES

[1] M. Alsabah *et al.*, "6G wireless communications networks: A comprehensive survey," *IEEE Access*, vol. 9, pp. 148191–148243, 2021, doi: 10.1109/ACCESS.2021.3124812.

[2] M. Shafi, R. K. Jha, and S. Jain, "6G: Technology evolution in future wireless networks," *IEEE Access*, vol. 12, pp. 57548–57573, 2024, doi: 10.1109/ACCESS.2024.3385230.

[3] Y. Lu and X. Zheng, "6G: A survey on technologies, scenarios, challenges, and the related issues," *Journal of Industrial Information Integration*, vol. 19, Sep. 2020, doi: 10.1016/j.jii.2020.100158.

[4] Z. Hu *et al.*, "Aiming for high-capacity multi-modal free-space optical transmission leveraging complete modal basis sets," *Optics Communications*, vol. 541, Aug. 2023, doi: 10.1016/j.optcom.2023.129531.

[5] M. Singh *et al.*, "A high-speed integrated OFDM/DPS-OCDMA-based FSO transmission system: Impact of atmospheric conditions," *Alexandria Engineering Journal*, vol. 77, pp. 15–29, Aug. 2023, doi: 10.1016/j.aej.2023.06.077.

[6] S. A. A. El-Mottaleb, H. Y. Ahmed, M. Zeghid, and A. S. A. O. Hassan, "Capacity enhancement based on using hybrid SCM with SAC-OCDMA using different codes for OFC and FSO transmission systems," *IEEE Access*, vol. 12, pp. 32462–32471, 2024, doi: 10.1109/ACCESS.2024.3366706.

[7] A. Bekkali, H. Fujita, and M. Hattori, "New generation free-space optical communication systems with advanced optical beam stabilizer," *Journal of Lightwave Technology*, vol. 40, no. 5, pp. 1509–1518, Mar. 2022, doi: 10.1109/JLT.2022.3146252.

[8] L. Li, N. Ji, Z. Wu, and J. Wu, "Design and experimental demonstration of an atmospheric turbulence simulation system for free-space optical communication," *Photonics*, vol. 11, no. 4, Apr. 2024, doi: 10.3390/photonics11040334.

[9] Y. Elsawy, A. S. Alatawi, M. Abaza, A. Moawad, and E.-H. M. Aggoune, "Next-generation dual transceiver FSO communication

system for high-speed trains in Neom smart city," *Photonics*, vol. 11, no. 5, May 2024, doi: 10.3390/photonics11050483.
[10] B.-S. Zhao, P.-F. Lv, and Y.-Q. Hong, "Channel correlation-based adaptive power transmission for free-space optical communications," *Photonics*, vol. 11, no. 9, Sep. 2024, doi: 10.3390/photonics11090859.
[11] A. M. Alhassan *et al.*, "Performance analysis of coherent source SAC OCDMA in free-space optical communication systems," *Symmetry*, vol. 15, no. 6, May 2023, doi: 10.3390/sym15061152.
[12] G. Park, V. Mai, H. Lee, S. Lee, and H. Kim, "Free-space optical communication technologies for next-generation cellular wireless communications," *IEEE Communications Magazine*, vol. 62, no. 3, pp. 24–30, Mar. 2024, doi: 10.1109/MCOM.001.2300160.
[13] M. Singh, M. H. Aly, and S. A. A. El-Mottaleb, "Performance analysis of 6 × 10 Gbps PDM-SAC-OCDMA-based FSO transmission using EDW codes with SPD detection," *Optik*, vol. 264, Aug. 2022, doi: 10.1016/j.ijleo.2022.169415.
[14] J. Wang *et al.*, "Auxiliary management and control channel (AMCC) for coherent frequency-division multiplexing (FDM) PON," *IEEE Photonics Journal*, vol. 16, no. 3, pp. 1–9, Jun. 2024, doi: 10.1109/JPHOT.2024.3381867.
[15] Z. Du *et al.*, "90-m/660-Mbps underwater wireless optical communication enabled by interleaved single-carrier FDM scheme combined with sparse weight-initiated DNN equalizer," *Journal of Lightwave Technology*, vol. 41, no. 16, pp. 5310–5320, Aug. 2023, doi: 10.1109/JLT.2023.3262352.
[16] V. Mishra, R. Upadhyay, U. R. Bhatt, and A. Kumar, "DEC TDMA: A delay controlled and energy efficient clustered TDMA mechanism for FiWi access network," *Optik*, vol. 225, Jan. 2021, doi: 10.1016/j.ijleo.2020.164921.
[17] T. Umezawa *et al.*, "25-Gbaud 4-WDM free-space optical communication using high-speed 2-D photodetector array," *Journal of Lightwave Technology*, vol. 37, no. 2, pp. 612–618, Jan. 2019, doi: 10.1109/JLT.2018.2881979.
[18] F. El-Nahal, T. Xu, D. AlQahtani, and M. Leeson, "A bidirectional wavelength division multiplexed (WDM) free space optical communication (FSO) system for deployment in data center networks (DCNs)," *Sensors*, vol. 22, no. 24, Dec. 2022, doi: 10.3390/s22249703.
[19] X.-H. Huang *et al.*, "WDM free-space optical communication system of high-speed hybrid signals," *IEEE Photonics Journal*, vol. 10, no. 6, pp. 1–7, Dec. 2018, doi: 10.1109/JPHOT.2018.2881701.
[20] S. M. Ammar *et al.*, "Development of new spectral amplitude coding OCDMA code by using polarization encoding technique," *Applied Sciences*, vol. 13, no. 5, Feb. 2023, doi: 10.3390/app13052829.
[21] M. Rahmani, A. Cherifi, G. N. Sabri, M. I. Al-Rayif, I. Dayoub, and B. S. Bouazza, "Performance investigation of 1.5 Tb/s optical hybrid 2D-OCDMA/OFDM system using direct spectral detection based on successive weight encoding algorithm," *Optics & Laser Technology*, vol. 174, Jul. 2024, doi: 10.1016/j.optlastec.2024.110666.
[22] R. Li and A. Dang, "A novel coherent OCDMA scheme over atmospheric turbulence channels," *IEEE Photonics Technology Letters*, vol. 29, no. 5, pp. 427–430, Mar. 2017, doi: 10.1109/LPT.2017.2652727.
[23] H. Mrabet, A. Cherifi, T. Raddo, I. Dayoub, and S. Haxha, "A comparative study of asynchronous and synchronous OCDMA systems," *IEEE Systems Journal*, vol. 15, no. 3, pp. 3642–3653, Sep. 2021, doi: 10.1109/JSYST.2020.2991678.
[24] B.-C. Yeh, "Establishing a spectral optical CDMA system involving the use of two mutually orthogonal states of polarizations using 1-D two-distinct codes with two-code keying," *IEEE Access*, vol. 12, pp. 53018–53030, 2024, doi: 10.1109/ACCESS.2024.3386094.
[25] H. Y. Ahmed, M. Zeghid, M. M. Gasim, and S. A. A. El-Mottaleb, "Multi-dimensional sigma shift matrix (nD-SSM) code with adaptable transmitter-receiver architecture to support multiclass users for SAC-OCDMA system," *IEEE Access*, vol. 12, pp. 76919–76935, 2024, doi: 10.1109/ACCESS.2024.3403725.
[26] N. Savino, J. Leamer, R. Saripalli, W. Zhang, D. Bondar, and R. Glasser, "Robust free-space optical communication utilizing polarization for the advancement of quantum communication," *Entropy*, vol. 26, no. 4, Mar. 2024, doi: 10.3390/e26040309.
[27] E. Wijanto and C.-M. Huang, "Design of bipolar optical code-division multiple-access techniques using phase modulator for polarization coding in wireless optical communication," *Applied Sciences*, vol. 11, no. 13, Jun. 2021, doi: 10.3390/app11135955.
[28] H.-C. Cheng, E. Wijanto, T.-C. Lien, P.-H. Lai, and S.-P. Tseng, "Multiple access techniques for bipolar optical code division in wireless optical communications," *IEEE Access*, vol. 8, pp. 83511–83523, 2020, doi: 10.1109/ACCESS.2020.2991071.
[29] S.-P. Tseng, E. Wijanto, P.-H. Lai, and H.-C. Cheng, "Bipolar optical code division multiple access techniques using a dual electro-optical modulator implemented in free-space optics communications," *Sensors*, vol. 20, no. 12, Jun. 2020, doi: 10.3390/s20123583.
[30] H. M. R. Al-Khafaji, R. Ngah, S. A. Aljunid, and T. A. Rahman, "A new two-code keying scheme for SAC-OCDMA systems enabling bipolar encoding," *Journal of Modern Optics*, vol. 62, no. 5, pp. 327–335, Mar. 2015, doi: 10.1080/09500340.2014.978914.
[31] C. T. Yen, H. C. Cheng, Y. T. Chang, and W. B. Chen, "Performance analysis of dual unipolar/bipolar spectral code in optical CDMA systems," *Journal of Applied Research and Technology*, vol. 11, no. 2, pp. 235–241, Apr. 2013, doi: 10.1016/S1665-6423(13)71533-5.
[32] H. Mrabet, S. Mhatli, I. Dayoub, and E. Giacoumidis, "Performance analysis of AO-OFDM-CDMA with advanced 2D-hybrid coding for amplifier-free LR-PONs," *IET Optoelectronics*, vol. 12, no. 6, pp. 293–298, Dec. 2018, doi: 10.1049/iet-opt.2018.5042.
[33] N. Dong-Nhat, M. A. Elsherif, and A. Malekmohammadi, "Investigations of high-speed optical transmission systems employing absolute added correlative coding (AACC)," *Optical Fiber Technology*, vol. 30, pp. 23–31, Jul. 2016, doi: 10.1016/j.yofte.2016.01.013.
[34] N. Avlonitis, E. M. Yeatman, M. Jones, and A. Hadjifotiou, "Multilevel amplitude shift keying in dispersion uncompensated optical systems," *IEE Proceedings - Optoelectronics*, vol. 153, no. 3, pp. 101–108, Jun. 2006, doi: 10.1049/ip-opt:20050039.
[35] J. Park, Y. Kim, and D. Kim, "Accelerated statistical eye diagram estimation method for efficient signal integrity analysis," *IEEE Access*, vol. 11, pp. 132699–132707, 2023, doi: 10.1109/ACCESS.2023.3336568.

BIOGRAPHIES OF AUTHORS

Eddy Wijanto received his B.S. degree from the Department of Electrical Engineering at Krida Wacana Christian University, Indonesia, in 2005, his M.S. degrees from the Department of Electrical Engineering, Pelita Harapan University, Indonesia, in 2009, and his Ph.D. degrees from the Electro-Optical Engineering department at National Formosa University, Yunlin County, Taiwan, R.O.C, in 2021. He received his Professional Engineer from Atma Jaya Indonesia Catholic University, in 2023. He is currently an Associate Professor at the Department of Electrical Engineering, Krida Wacana Christian University, Indonesia. His major interests are mainly in the areas of wireless and optical communications. He can be contacted at email: eddy.wiyanto@ukrida.ac.id.

Kevin Sutanto received his B.S. degree from the Department of Electrical Engineering at Krida Wacana Christian University, Indonesia, in 2019, his M.S. degree from the Department of Electronics Engineering, Ming-Chi University of Technology, Taiwan, in 2022. He is currently a Lecturer at the Department of Electrical Engineering, Krida Wacana Christian University, Indonesia. His major interests are mainly in the areas of artificial intelligence and computer vision. He can be contacted at email: kevin.sutanto@ukrida.ac.id.